

This is a pre-print of an article published in *Applied Microbiology and Biotechnology*. The final authenticated version is available online at: <https://doi.org/10.1007/s00253-018-8737-7>

[Click here to view linked References](#)

Hydrogen metabolic patterns driven by *Clostridium-Streptococcus* community shifts in
a continuous stirred tank reactor

Rodolfo Palomo-Briones¹, Eric Trably², Nguyen Esmeralda López-Lozano¹, Lourdes B.
Celis¹, Hugo Oscar Méndez-Acosta³, Nicolas Bernet², Elías Razo-Flores^{1*}

¹División de Ciencias Ambientales, Instituto Potosino de Investigación Científica y
Tecnológica. Camino a la Presa San José 2055, Lomas 4a Sección, C.P. 78216, San Luis
Potosí, S.L.P., México

²LBE, INRA, Univ Montpellier, 102 avenue des Etangs, 11100 Narbonne, France

³Departamento de Ingeniería Química, CUCEI-Universidad de Guadalajara, Blvd. M.
García Barragán 1451, C.P. 44430, Guadalajara, Jal., México

*Corresponding author: erazo@ipicyt.edu.mx
+ 52 (444) 8342026

ORCID IDs:

Rodolfo Palomo-Briones: 0000-0002-7164-0756

Nicolas Bernet: 0000-0003-2710-3547

Elías Razo-Flores: 0000-0002-8262-695X

ACKNOWLEDGEMENTS

This research was financially supported by the Fondo de Sustentabilidad Energética
SENER-CONACYT, Clúster Biocombustibles Gaseosos (project 247006). Rodolfo Pal-
omo-Briones is thankful for the PhD scholarship provided by CONACYT. The authors
acknowledge the technical help of Gaëlle Santa-Catalina, Dulce Partida Gutiérrez,
Guillermo Vidriales Escobar, and Juan Pablo Rodas Ortiz. The infrastructure provided
by CONACYT INFR-2014-01-224220 is also acknowledged.

ABSTRACT

1
2 The hydrogen production efficiency in dark fermentation systems is strongly dependent
3 on the occurrence of metabolic pathways derived from the selection of microbial species
4 that either consume molecular hydrogen or outcompete hydrogenogenic bacteria for the
5 organic substrate. In this study, the effect of organic loading rate (OLR) on the
6 hydrogen production performance, the metabolic pathways and the microbial
7 community composition in a continuous system was evaluated. Two bacterial
8 populations, *Clostridium* and *Streptococcus*, were dominant in the microbial community
9 depending on the OLR applied. At low OLR (14.7 - 44.1 g_{Lactose}/L-d), *Clostridium sp.*
10 was dominant and directed the system towards the acetate-butyrate fermentation
11 pathway, with a maximum H₂ yield of 2.14 mol_{H₂}/mol_{Hexose} obtained at 29.4 g_{Lactose}/L-d.
12 Under such conditions, the volumetric hydrogen production rate (VHPR) was between
13 3.2 - 11.6 L_{H₂}/L-d. In contrast, high OLR (58.8 and 88.2 g_{Lactose}/L-d) favored the
14 dominance of *Streptococcus sp.* as co-dominant microorganism leading to lactate
15 production. The formate production was also stimulated under these conditions possibly
16 through the Wood-Ljungdahl pathway as strategy to dispose the surplus of reduced
17 molecules (e.g. NADH₂⁺), which theoretically consumed up to 5.72 L_{H₂}/L-d. Under
18 such scenario, the H₂ yield was relatively low (0.74 mol_{H₂}/mol_{Hexose} at OLR = 58.8
19 g_{Lactose}/L-d) regardless of the higher VHPR reached (13.7 – 14.5 L_{H₂}/L-d). Overall, this
20 research brings clear evidence of the intrinsic occurrence of metabolic pathways
21 detrimental for hydrogen production, *i.e.* lactic acid fermentation and formate
22 production, during hydrogen production, suggesting the use of low OLR as strategy to
23 control such undesirable metabolisms.
24
25
26
27
28
29
30
31
32
33
34
35
36
37
38
39
40
41
42
43
44

KEYWORDS

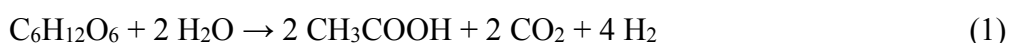
45 Biohydrogen; Dark fermentation; Lactic Acid Bacteria (LAB); Hydrogen-producing
46 bacteria (HPB): microbial community
47
48
49
50
51
52
53
54
55
56
57
58
59
60
61
62
63
64
65

INTRODUCTION

The development of zero- and low-carbon technologies for energy production is an important milestone in the mitigation of climate change. In this regard, biofuels have gained great attention due to the possibility to revalorize organic wastes generated by industrial, agricultural, and domestic sectors, and minimize the release of additional carbon into the atmosphere.

Biohydrogen (H₂) is an energy carrier that can be distinguished among other fuels due to its high-energy content (120 kJ/g), highly efficient conversion to electric energy, and byproducts-free oxidation. The production of biohydrogen can be performed through four major biological processes: direct and indirect biophotolysis, photofermentation and dark fermentation. Among these, the dark fermentative technology has shown higher production rates and faster and simpler operation than its counterparts. Moreover, dark fermentation is independent of light and the microbial communities have a wide potential to metabolize many types of organic wastes by showing a good performance in spite to fluctuations of environmental conditions through metabolic flexibility (Azwar et al. 2014).

Theoretically, the maximum hydrogen metabolic yield of dark fermentative systems is four moles of H₂ per mole of glucose consumed (Agler et al. 2011). This yield is possible to achieve if only *Clostridium* species are involved in the fermentation by producing acetate as byproduct (Eq. 1).



In practice, H₂ yields are substantially lower than the theoretical value by considering the ideal acetate fermentation (Nath and Das 2004). This is mainly due to the diversity of metabolic routes, i.e., the production of metabolites associated with low or none H₂ production. Such is the case of butyrate, propionate, ethanol, and lactate pathways, among others. Special focus has been paid on the lactate production, which is performed by lactic-acid bacteria (LAB) such as *Lactobacillus*, *Sporolactobacillus*, *Streptococcus*, etc. LAB outcompete hydrogenogenic microorganisms for the carbon source, but are also capable to produce growth-inhibitory compounds (Noike et al. 2002; Sikora et al. 2013; Gomes et al. 2016). Recently, it was reported for continuous stirred tank reactors (CSTR) fed with lactose that LAB co-dominated at large hydraulic retention times (HRT = 18 and 24 h). As consequence, short values of retention time (HRT = 6 and 12

1 h) were suggested as strategy to control the proliferation of LAB (Palomo-Briones et al.
2 2017). However, to the best of our knowledge, the effects of the OLR at fixed HRT on
3 LAB in a dark fermentative environment remain unexplored in CSTR systems. This
4 issue is of high interest since the relationship between OLR and LAB can potentially
5 affect the scaling up and economy of the process. On the other hand, H₂ yield can also
6 be shortened due to H₂ consumption through the Wood-Ljungdahl pathway (WLP),
7 which can be carried out by several *Clostridium* species (Diekert and Wohlfarth 1994;
8 Saady 2013). In such pathway, H₂ and CO₂ are combined to produce acetyl-CoA and a
9 diversity of other metabolites (Diekert and Wohlfarth 1994; Tracy et al. 2012;
10 Schuchmann and Müller 2014).

11 Different authors have reported that LAB and WLP-hydrogenotrophic microorganisms
12 are affected by environmental and operational conditions (e.g. Shanmugam et al. 2014;
13 Carrillo-Reyes et al. 2014; Si et al. 2015). Nevertheless, most studies have been focused
14 on the suppression of either LAB or WLP-hydrogenotrophic microorganisms, although
15 these could be simultaneously present. Under such scenario, the strategies aimed to
16 suppress one of these groups could result in the enrichment of the second one, and *vice*
17 *versa*. Therefore, this work aims to investigate the effect of OLR on the performance of
18 H₂ production, metabolic pathways and microbial community in a lactose fed CSTR,
19 with special focus on the potential co-occurrence of LAB and WLP-hydrogenotrophic
20 microorganisms.

21 MATERIALS AND METHODS

22 Inoculum and substrate

23 Anaerobic granular sludge from a full-scale UASB reactor treating wastewater from a
24 tequila factory was used as inoculum. Before inoculation, the sludge was disaggregated
25 and heat pretreated at 90-95 °C for 2 hours. The inoculum was added at a final
26 concentration of 4.5 g volatile suspended solids (VSS)/L. Cheese whey powder (CWP)
27 (Darigold, USA) with lactose content of 75.5% was used as substrate at concentrations
28 ranging from 3.7 to 22.5 g_{lactose}/L. The feeding solution was supplemented with (mg/L):
29 NH₄Cl, 2100; MgCl₂·6H₂O, 100; CuCl₂·H₂O, 1.25; MnCl₂ 4H₂O, 7; FeCl₂ 4H₂O, 19.1;
30 NiCl₂ 6H₂O, 102.5. Additionally, phosphate buffer (KH₂PO₄-Na₂HPO₄, pH 5.9) was
31 added to a final concentration of 100 mM.

32 2.2. Experimental setup

1 A bioreactor made of glass, with 1 L working volume and 0.3 L of head space
2 (APPLIKON Biotechnologies, USA) was inoculated with the heat pretreated anaerobic
3 sludge. The system was started-up in batch mode for 24 h using CWP at a concentration
4 of 22 g_{Lactose}/L. Afterwards, the reactor was shifted to continuous operation at a HRT of
5 6 h (OLR of 88 g_{Lactose}/L-d). In subsequent stages, the OLR was decreased gradually
6 from 88 to 15 g_{Lactose}/L-d by modifying the CWP concentration. Stirring, hydraulic
7 retention time, temperature and pH were set and controlled at 250 rpm, 6 h, 37 °C and
8 5.9, respectively.
9

10 Analytical methods

11 Liquid samples were collected in a regularly basis and used to determine biomass,
12 chemical oxygen demand (COD), total carbohydrates and volatile fatty acids (VFA).
13 Biomass (as volatile suspended solids, VSS) and soluble COD were quantified as
14 described in the standard methods (APHA/AWWA/WEF 2012). Total carbohydrates
15 were determined by the phenol sulfuric method (Dubois et al. 1956). VFA were
16 quantified from filtered (0.22 mm) samples by capillary electrophoresis (1600A, Agilent
17 Technologies, Waldbronn, Germany) as reported elsewhere (Davila-Vazquez et al.
18 2008).
19

20 The volume of gas produced was measured through a liquid displacement device, and
21 its composition (H₂ and CO₂) was determined through a gas chromatograph equipped
22 with a thermal conductivity detector (6890N, Agilent Technologies, Waldbronn,
23 Germany). All the gas volumes are reported at 1 atm and 273.15 K.
24

25 2.4 Capillary Electrophoresis - Single Strand Conformation Polymorphism (CE-SSCP)

26 The CE-SSCP was performed as described elsewhere (Palomo-Briones et al. 2017). In
27 brief, the bacterial DNA was extracted using the ZR Fungal/Bacterial DNA MiniPrep
28 extraction kit according to manufacturer's instructions (Zymo Research). The
29 amplification of the V3 region of the 16S rRNA genes was performed with Pfu Turbo
30 DNA polymerase (Stratagene, La Jolla, CA, USA) and the universal primers W49 5'-
31 ACGGTCCAGACTCCTACGGG -3' and W104 5'- TTACCGCGGCTGCTGGCAC -3'.
32 The PCR conditions were set as follows (Milferstedt et al. 2013): initial denaturation for
33 2 min at 94°C; 25 cycles of melting (1 min at 94°C), annealing (1 min at 61°C) and
34 extension (1 min at 72°C); and a final extension step of 10 min at 72°C.
35

36 The PCR products were analyzed by CE-SSCP in an ABI 3130 genetic analyzer
37
38
39
40
41
42
43
44
45
46
47
48
49
50
51
52
53
54
55
56
57
58
59
60
61
62
63
64
65

1 (Applied Biosystems, Foster City, CA, USA) as reported by Rochex et al. (2008). The
2 resulting CE-SSCP profiles were aligned with an internal standard (ROX) to consider
3 the inter-sample electrophoretic variability and were normalized with the package
4 *Statfingerprints* available on R platform (R Development Core Team 2011).
5
6

7 The relative abundances of each peak on CE-SSCP profiles were computed with the
8 spectroscopy functionality of OriginPro 8 (first derivative method, both directions, min
9 height 1%, min width 1%). Subsequently, a Pearson's distances matrix was computed
10 using CE-SSCP relative abundances, and it was displayed as a hierarchical cluster
11 dendrogram. Such computing was carried out with the *corrplot*, *ggplot* and *ggdendro*
12 packages under R environment (R Development Core Team 2011).
13
14
15
16
17
18

19 Illumina sequencing and microbial community analysis

20
21
22 Illumina MiSeq 2x250 paired-end sequencing was performed following the
23 manufacturers protocol (Illumina, USA). The V3-V4 regions of the rRNA gene (~450
24 bp) were amplified with the primers 341F (5'-CCTACGGGNGGCWGCAG) and 805R
25 (5'-GACTACHVGGGTATCTAATCC) fused with Illumina adapters. The polymerase
26 chain reaction (PCR) was performed using the Phusion High-Fidelity PCR Master Mix
27 with HF Buffer (Thermo Scientific, USA) and the following conditions: initial
28 denaturation step at 95 °C for 3 min, followed by 25 cycles (95 °C, 30 sec; 55 °C, 30
29 sec; 72 °C, 30 sec) and a final elongation step at 72 °C for 5 min. The PCR products
30 were indexed with Nextera XT index primers in a second PCR (8 cycles) under identical
31 conditions. The resulting amplicons were purified with Agencourt AMPure XP beads
32 (Beckman Coulter, USA) and re-suspended in Illumina buffer. The Illumina sequencing
33 work was carried out by the Unidad Universitaria de Secuenciación Masiva y
34 Bioinformática, Instituto de Biotecnología, UNAM, Cuernavaca, Morelos, México.
35
36
37
38
39
40
41
42
43
44
45

46 The downstream sequence processing was performed using the Quantitative Insights
47 into Microbial Ecology (QIIME) software (Caporaso et al. 2010). The analysis included
48 the merging of the paired sequences with a minimum overlapping of 20 bp and zero
49 errors in the overlapping region. The resulting sequences were quality filtered at a Phred
50 score > Q20. Sequences with less than 350 pb were also eliminated. The chimeric
51 sequences were filtered with the UCHIME 6.1 software (Edgar et al. 2011). Afterwards,
52 open OTU picking at a 97% sequence identity was carried out with the UCLUST
53 algorithm (Edgar 2010) using the SILVA RNA database (128 release) as reference
54
55
56
57
58
59
60
61
62
63
64
65

(<https://www.arb-silva.de/download/archive/qiime/>). The sequences of this work were deposited in the NCBI BioProject PRJNA392772.

RESULTS

Dark fermentation performance

The CSTR was operated during 80 days under controlled pH (5.9), temperature (37 °C) and HRT (6 h). The reactor was fed at six sequential OLR: 88, 59, 44, 29, 22, and 15 g_{lactose}/L-d, referred from now on as Stage I, Stage II, Stage III, Stage IV, Stage V, and Stage VI, respectively. After the first six stages were carried out, an unexpected low performance was noticed in Stage II; thus, the OLR of 59 g_{lactose}/L-d was applied again after Stage VI (15 g_{lactose}/L-d). In total, the experiments consisted of seven experimental phases as shown in Fig. 1a.

The performance results show that the volumetric hydrogen production rate (VHPR) was directly linked with the OLR (Fig. 1a). A maximal VHPR of 13.9 ± 2.2 L_{H₂}/L-d (mean \pm SD) was observed in Stage I (OLR of 88.2 g_{Lactose}/L-d), while the lowest VHPR of 3.04 ± 0.9 L_{H₂}/L-d was found in Stage VI (OLR of 14.7 g_{Lactose}/L-d). This confirmed that a successful hydrogenogenic fermentation was established. In terms of H₂ yield, the optimal value of 2.17 ± 0.29 mol_{H₂}/mol_{Hexose} (mean \pm SD) was found at an OLR of 29.4 g_{Lactose}/L-d (Stage IV). Overall, the H₂ yields ranged between 0.67 and 2.17 mol_{H₂}/mol_{Hexose} (Fig. 1b).

To determine the main metabolic pathways along the experiment, the VFA were also quantified through capillary electrophoresis. In terms of molar yield, steady state values of acetate and butyrate ranged within 0.13 - 0.53 mol_{Acetate}/mol_{Hexose} and 0.26 - 0.78 mol_{Butyrate}/mol_{Hexose}, respectively. On the other hand, the steady state values of formate and lactate were between 0.07 - 0.51 mol_{Formate}/mol_{Hexose} and 0.03 - 0.59 mol_{Lactate}/mol_{Hexose}, respectively. Further analysis of the steady states revealed positive correlations between the H₂ yield and the molar yields of acetate and butyrate (Fig. S1, b and d). On the contrary, the molar yields of acetate and butyrate were negatively correlated with the OLR (Fig. S1, f and h). It is worth to mention that during the operation of the CSTR, acetate and butyrate were produced in a roughly constant acetate/butyrate ratio of 0.7, independently of OLR, VHPR and H₂ yield. Moreover, the

1 H₂ yield was negatively associated with lactate and formate yields (Fig. S1, a and c).
2 The data show that the metabolic routes associated with these two compounds seemed
3 to be favored at relatively high OLR (59 and 88 g_{Lactose}/L-d) (Fig. S1, e and g).
4

5
6 Considering that the synthesis of one mole of formate implies the direct or indirect
7 consumption of one mole of H₂, the amount of H₂ depleted in such route was estimated.
8 As result, the maximum amount of H₂ converted to formate was equivalent to 5.7
9 L_{H₂}/L-d at an OLR of 88 g_{Lactose}/L-d (Stage I). In contrast, the stage with the minimum
10 production of formate was Stage IV (OLR = 29 g/L-d) during which the equivalent
11 amount of H₂ depleted was of 0.25 ± 0.08 L_{H₂}/L-d. Consistently, the maximum H₂ yield
12 was also presented at the same experimental stage (Table 1).
13
14
15
16
17
18

19 Microbial community analysis

20 16S-rRNA amplicons obtained at steady states were analyzed by CE-SSCP to
21 characterize the microbial community structure and reveal the OLR-associated changes.
22 The analysis showed that during the CSTR operation the microbial community was
23 composed principally by three different microorganisms numbered 150, 224 and 910 in
24 reference to the SSCP retention time (Fig. 2b). Based on relative abundances, the
25 microorganism numbered 910 was dominant at OLR ≥ 59 g_{Lactose}/L-d. In contrast, two
26 different organisms (150 and 224) dominated at OLR ≤ 44 g_{Lactose}/L-d. An Unweighted
27 Pair Group Method with Arithmetic Mean (UPGMA) analysis of the CE-SSCP profiles
28 showed a clear association among stages I, II and VII, regardless of the amount of time
29 separating such experimental stages (Fig. 2a). On the other hand, stages III, IV, V and
30 VI were also clustered with each other. Overall, two cohesive and OLR-dependent
31 microbial community groups were unveiled.
32
33
34
35
36
37
38
39
40
41
42
43

44 To identify the microbial genera involved in the fermentation, the V3-V4 regions of
45 16S-rRNA gene were sequenced and compared with the Silva 16S RNA database to
46 assign taxonomy. The 16S RNA sequencing resulted in 664101 ± 67239 high quality
47 reads per sample, grouped in 14559 operational taxonomic units (OTU), identified up to
48 the genus level. Overall, the results showed the presence of two main genera that
49 dominated all along the fermentation time, *Clostridium* and *Streptococcus* (Fig. 3). To
50 identify and characterize the link between CE-SSCP and 16S-rRNA sequencing, a
51 correlation analysis was conducted. The results showed that *Clostridium* was well
52 correlated with microorganisms numbered 150 (R²=0.96, p<0.01) and 224 (R²=0.96,
53 p<0.01) while *Streptococcus* was strongly correlated with the microorganism numbered
54
55
56
57
58
59
60
61
62
63
64
65

1
2
3
4
5
6
7
8
9
10
11
12
13
14
15
16
17
18
19
20
21
22
23
24
25
26
27
28
29
30
31
32
33
34
35
36
37
38
39
40
41
42
43
44
45
46
47
48
49
50
51
52
53
54
55
56
57
58
59
60
61
62
63
64
65

910 ($R^2=0.98$, $p<0.01$). Therefore, 16S-rRNA sequencing results were utilized for microbial community analysis.

As shown in Fig. 3, *Clostridium* and *Streptococcus* accounted for more than 88% of the relative abundance, while other microbial genera such as *Enterobacter*, *Escherichia*, *Lactobacillus*, *Lactococcus* and *Enterococcus*, remained subdominant. In general, the relative abundance of *Clostridium* was strongly associated with the reduction of the OLR, while the *Streptococcus* abundance was higher as the OLR increased (Fig. 3b).

In order to better understand and visualize the relationship between the microbial community composition and the performance of the reactor (i.e. VHPR, OLR, H₂ yield, and VFA yields), a Principal Components Analysis (PCA) was conducted (Fig. 4). Two principal components accounted for more than 80 percent of the dataset variance. The results showed a clear relationship between *Clostridium* and the butyrate and acetate yields. On the other hand, *Streptococcus* was strongly linked to VHPR, OLR, and lactate yield. Interestingly, formate and H₂ yields showed negative influence on each other, confirming the aforementioned negative correlation between these two metabolic products. Nevertheless, no linear relationship was found between formate and H₂ yields with the *Clostridium* nor *Streptococcus* abundance.

DISCUSSION

The continuous H₂ production from CWP was successfully established in a continuous reactor and was comparable to previous works under similar conditions (Davila-Vazquez et al. 2009; Cota-Navarro et al. 2011). Davila-Vazquez et al. (2009) reported a VHPR of 12.5 L_{H2}/L-d at an OLR of 92.4 g_{Lactose}/L-d, while Cota-Navarro et al. (2011) reported a VHPR of 16.1 L_{H2}/L-d at an OLR of 95 g_{Lactose}/L-d. Both values were quite similar to the VHPR found in this research (13.7 ± 1.3 L_{H2}/L-d at an OLR of 88 g_{Lactose}/L-d) and demonstrate the reliability and reproducibility of dark fermentation with CSTR systems.

Next generation sequencing analysis revealed that a low diverse and highly specialized microbial community composed mainly by *Clostridium* and *Streptococcus* drove the lactose-based dark-fermentative hydrogen production in the CSTR. Such a low microbial diversity was previously described as a common characteristic of hydrogen-producing bioreactors (Etchebehere et al. 2016). This feature becomes accentuated due

to the strong selection pressure that is typical of suspended-growth systems.

Interestingly, the relative abundances of these genera were negatively associated to each other, suggesting competitive interactions. In addition, the changes in the OLR had a critical impact on the microbial community distribution and subsequent metabolites production, including H₂. In this regard, two different OLR-dependent states of operation were identified.

Highly efficient H₂ producing phase

The operation of the dark fermentative CSTR under $OLR \leq 44.1 \text{ g}_{\text{Lactose}}/\text{L-d}$ was found to favor the efficiency of H₂ production, i.e. the H₂ yield. At such conditions (Stages III-VI), the microbial community was clearly dominated by microorganisms from the *Clostridium* genera (Fig. 3). These microorganisms have been widely found in dark fermentative systems and have been identified as highly desirable species for H₂ production (Cabrol et al. 2017). Theoretically, *Clostridium* species are capable to produce H₂ with a metabolic yield of $4 \text{ mol}_{\text{H}_2}/\text{mol}_{\text{Hexose}}$ following the acetate pathway (Eq. 1). However, this route is only feasible at low H₂ partial pressures ($P_{\text{H}_2} < 60 \text{ Pa}$); otherwise, the synthesis of H₂ from NADH becomes thermodynamically unfavorable (Angenent et al. 2004). *Clostridium* microorganisms can also perform the synthesis of H₂ through the butyrate pathway ($\text{C}_6\text{H}_{12}\text{O}_6 \rightarrow \text{CH}_3\text{-CH}_2\text{-CH}_2\text{-COOH} + 2 \text{ CO}_2 + 2\text{H}_2$) which leads to a theoretical H₂ yield of $2 \text{ mol}_{\text{H}_2}/\text{mol}_{\text{Hexose}}$. These two pathways (acetate and butyrate) are considered as the most efficient pathways for H₂ production through the dark fermentative process.

In agreement, acetate and butyrate were the principal VFA produced under the dominance of *Clostridium* genera (Fig. 2c); the H₂ yield reached a maximum mean value of $2.14 \text{ mol}_{\text{H}_2}/\text{mol}_{\text{Hexose-consumed}}$ (Stage IV). Considering the metabolic limitation and that most of literature has reported H₂ yields of about $1.3 \text{ mol}_{\text{H}_2}/\text{mol}_{\text{Hexose}}$, the results of the present study at $OLR \leq 44.1 \text{ g}_{\text{Lactose}}/\text{L-d}$ are quite remarkable. On the other hand, the VHPR ($3.2 - 11.6 \text{ L}_{\text{H}_2}/\text{L-d}$) was still low, compared to that reported in other studies (Davila-Vazquez et al. 2009; Lee et al. 2012; Sivagurunathan and Lin 2016). The increase of the OLR could possibly lead to higher VHPR but, as discussed in the following section, the increase of the organic loading rate could cause new problems that have significant impacts on the efficiency of the process.

Lactate and formate favored at high OLR

1 The operation of the CSTR at $OLR \geq 58.8 \text{ g}_{\text{Lactose}}/\text{L-d}$ caused an important increase in
2 the VHPR (12.3 - 14.5 L/L-d) while the efficiency of the process was notably reduced
3 (1.21 - 1.9 mol_{H₂}/mol_{Hexose}). This seems to be a disjunction point between productivity
4 and efficiency of hydrogen production. A possible explanation for such phenomenon is
5 that, under high OLR conditions, H₂ is produced in such an amount that probably it is
6 not transferred off the system with the required efficiency, i.e. the process is limited by
7 mass transfer. Under such conditions, the microorganisms pursue alternative pathways
8 to dispose the electrons gathered from the organic substrate and tend to produce less H₂
9 (Nath and Das 2004). The results clearly showed that the alternative metabolic routes
10 were lactate and formate production.
11

12 The presence of lactate is a clear signal of the occurrence of lactic acid fermentation,
13 which is usually found in dark fermentative systems (Baghchehsaraee et al. 2010;
14 Sikora et al. 2013; Etchebehere et al. 2016). Such finding was confirmed by the
15 presence of *Streptococcus*, a lactic acid bacterium that was mainly present at relatively
16 high OLR (Fig. 3). *Streptococcus* has been previously found inside hydrogenogenic
17 granules where they presumably strengthen the granule structure (Hung et al. 2011).
18 Davila-Vazquez et al. (2009) also reported the presence of *Streptococcus* in a CSTR fed
19 with lactose-CWP at an OLR of 92.4 and 138.6 g_{Lactose}/L-d with HRT of 6 h and 4 h,
20 respectively. In a recent report, it was concluded that the HRT is a factor of selection
21 that strongly affects the microbial community composition; it was shown that LAB
22 (*Streptococcaceae* and *Sporolactobacillaceae*) could be eliminated at low HRT (6 h)
23 (Palomo-Briones et al. 2017). In the present work, although the HRT was maintained at
24 6 h, the elimination of LAB was only possible when using low OLR values.
25

26 The microbial community dynamics is often associated to the differences in growth
27 capabilities of the involved species. However, in the case of LAB and *Clostridium*,
28 different studies have reported similar Monod-type growth kinetics (in terms of μ_{max} and
29 K_s) with lactose (Table 2); therefore, the community behavior observed in the present
30 study could be barely explained by kinetic differences. Rather, the community structure
31 could be the result of product inhibitory effects over *Clostridium* at high OLR that
32 allowed LAB to better compete for the substrate uptake. Napoli et al. (2011) reported
33 that *Clostridium acetobutylicum* could be inhibited by the accumulation of acetate and
34 butyrate, with critical concentrations of 26 mmol/L and 34 mmol/L, respectively. In the
35 present study, the acetate and butyrate concentrations were in the range of those
36
37
38
39
40
41
42
43
44
45
46
47
48
49
50
51
52
53
54
55
56
57
58
59
60
61
62
63
64
65

1 reported as inhibitory by Napoli et al., (2011) and strongly associated with the OLR,
2 reaching their highest concentrations at OLR of 88.2 g_{Lactose}/L-d (Table 1). On the
3 contrary, the lowest concentrations of acetate and butyrate were observed at OLR of 15
4 g_{Lactose}/L-d, where *Clostridium* was strongly dominant. Therefore, the inhibition
5 phenomenon seems to be an important driver of the *Clostridium-Streptococcus*
6 dynamics.
7
8
9

10 Considering the microbial community results, the formate synthesis was probably
11 performed by *Clostridium* species. Theoretically, the production of formate is carried
12 out with the catalysis of the pyruvate:formate lyase (*pfl*) and the formate dehydrogenase
13 (*fdh*). The former enzyme catalyzes the activation of pyruvate to acetyl-CoA with the
14 concomitant production of formate and CO₂, while the later catalyzes the synthesis of
15 formate from NADH₂⁺ and CO₂. The *pfl* is broadly found in facultative anaerobes, but it
16 has been also found in the genome of different *Clostridium* species such as *C.*
17 *butyricum*, *C. acetobutylicum*, *C. beijirinkii*, *C. pasteurianum*, and *C. tyrobutyricum*
18 (Nölling et al. 2001; Pyne et al. 2014; Noar et al. 2014; Kwok et al. 2014; Lee et al.
19 2016)
20
21
22
23
24
25
26
27
28

29 In addition, the gene of *fdh* enzyme has been reported to be part of the genome of
30 different *Clostridium* species, such as *C. carboxidivorans* (Bruant et al. 2010), *C.*
31 *ljungdahlii* (Köpke et al. 2010), *C. beijirinkii* (Milne et al. 2011), and *C. acetobutylicum*
32 (Senger and Papoutsakis 2008). *fdh* is also the first enzyme to participate in the WLP
33 which leads to the synthesis of acetate (homoacetogenesis). Considering the actual
34 concentrations of VFA, acetate and formate synthesis from H₂ and CO₂ are both
35 favorable reactions (Table 3). Nevertheless, no evidence of autotrophic acetate
36 (homoacetogenesis) was found in the experiments here reported. Therefore, formate was
37 probably the main hydrogen sink under the conditions tested.
38
39
40
41
42
43
44
45
46

47 To determine the exact mechanism of formate production will require further studies.
48 However, as formate was OLR dependent, our hypothesis is that such conditions caused
49 an excess of reduced equivalents (NADH₂⁺, Fd_{red}) that accumulated in the cell due to
50 kinetic limitation at the hydrogenases (*hyd*) level. The primary method to dispose
51 electrons is by the action of hydrogenases, but their activity is retro-inhibited at high
52 concentrations of H₂. Thus, the production of formate was a possible strategy to dispose
53 the excess of electrons gathered from the organic substrate, and maintain NAD⁺/NADH
54 and Fd_{ox}/Fd_{red} equilibriums. Under this hypothesis, not only homoacetogenesis but also
55
56
57
58
59
60
61
62
63
64
65

1 formic acid synthesis through either the *fdh* (i.e. WLP) or *pfl* route plays an important
2 role in H₂ consumption that deserves to be studied with detail.

3
4 To overcome the detrimental consequences of formate synthesis and boost hydrogen
5 production, new ways to recover H₂ (and possibly CO₂ as well) as soon as it is produced
6 should be developed and implemented. In this regard, different alternatives have been
7 proposed with the aim to increase H₂ productivities. Nasr et al. (2015) reported 22%
8 increase of H₂ yield using KOH pellets to capture CO₂ *in situ*. The capture of CO₂, as
9 discussed by the authors, favored the shift of the hydrogenogenic reactions to the
10 forward direction (i.e. production of H₂). Moreover, CO₂ sequestration also had an
11 influence on the metabolic pathways, favoring acetate productivity while lowering
12 butyrate production. Other researchers conducted experiments under a continuous
13 release of biogas generated maintaining the headspace pressure at or below of 0.116 atm
14 (Esquivel-Elizondo et al. 2014). They found that under such conditions the system
15 enhanced in terms of H₂ yield (from 1.2 to 1.9 mol H₂ /mol_{glucose}) and VHPR (from 36 to
16 108 mL H₂/L-h) in comparison to their control (gas released when pressure was above
17 1.36 atm).

18
19 Overall, this research shows the results of continuous H₂ production in a CSTR from
20 cheese whey powder as substrate. The microbial community was dominated by three
21 bacterial phylotypes from two main genera, *Clostridium* and *Streptococcus*, whose
22 relative abundances were strongly affected by the OLR. The shift in the microbial
23 community composition also influenced the metabolic pathways performed. At low
24 OLR (14.7-44.1 g_{Lactose}/L-d), *Clostridium* was the dominant genus and drove the system
25 to a highly efficient acetate-butyrate fermentation with a maximum H₂ yield of 2.14
26 mol_{H₂}/mol_{Hex-consumed} obtained at an OLR of 29.4 g_{Lactose}/L-d. In contrast, high OLR
27 (58.8 and 88.2 g_{Lactose}/L-d) caused an increase of acetate and butyrate concentrations,
28 which possibly inhibited *Clostridium* growth and prompted the competition of LAB.
29 Under such scenario, *Streptococcus* aroused as the co-dominant microorganism and was
30 successfully associated with the production of lactate. In consequence, the efficiency of
31 H₂ production was negatively affected (min H₂ yield=0.74 mol_{H₂}/mol_{Hexose} at OLR=58.8
32 g_{Lactose}/L-d) regardless of the higher VHPR observed (max 13.7 L/L-d) in comparison
33 with low OLR conditions. Moreover, it was found that H₂ was probably consumed
34 through metabolic pathways leading to the production of formate as alternative to
35 dispose the excess of reduced equivalents. Most probably, either the *pfl* or *fdh* (through
36
37
38
39
40
41
42
43
44
45
46
47
48
49
50
51
52
53
54
55
56
57
58
59
60
61
62
63
64
65

1 the WLP) were possible involved in such phenomenon. Thus, not only
2 homoacetogenesis but also formic acid synthesis plays an important role in H₂
3 consumption has and deserves to be studied with detail. A whole analysis of the results
4 of this research revealed that the detrimental metabolisms of lactic acid fermentation
5 and formate synthesis could be minimized at low OLR. Otherwise, the effective
6 liberation of H₂ right after its production will be also required.
7
8
9

10 11 12 13 CONFLICT OF INTEREST

14 The authors declare that they have no conflict of interest.
15
16
17
18
19

20 21 ETHICAL STATEMENT

22 The authors confirm that the article does not contain any studies with human
23 participants or animals.
24
25
26
27
28

29 30 SUPPORTING INFORMATION AVAILABLE

31 Additional supporting information is available in the online version of this article at the
32 publisher's web-site.
33
34
35
36

37 38 REFERENCES

39 Agler MT, Wrenn B a, Zinder SH, Angenent LT (2011) Waste to bioproduct conversion
40 with undefined mixed cultures: the carboxylate platform. *Trends Biotechnol*
41 29:70–78. doi: 10.1016/j.tibtech.2010.11.006
42
43

44 Altiok D, Tokatli F, Harsa S (2006) Kinetic modelling of lactic acid production from
45 whey by *Lactobacillus casei* (NRRL B-441). *J Chem Technol Biotechnol* 81:1190–
46 1197. doi: 10.1002/jctb.1512
47
48
49

50 Angenent LT, Karim K, Al-Dahhan MH, Wrenn B a., Domínguez-Espínosa R (2004)
51 Production of bioenergy and biochemicals from industrial and agricultural
52 wastewater. *Trends Biotechnol* 22:477–485. doi: 10.1016/j.tibtech.2004.07.001
53
54

55 APHA/AWWA/WEF (2012) *Standard Methods for the Examination of Water and*
56 *Wastewater*.
57
58

59 Azwar MY, Hussain M a., Abdul-Wahab AK (2014) Development of biohydrogen
60
61
62
63
64
65

1 production by photobiological, fermentation and electrochemical processes: A
2 review. *Renew Sustain Energy Rev* 31:158–173. doi: 10.1016/j.rser.2013.11.022
3
4 Baghchehsaraee B, Nakhla G, Karamanev D, Margaritis A (2010) Fermentative
5 hydrogen production by diverse microflora. *Int J Hydrogen Energy* 35:5021–5027.
6 doi: 10.1016/j.ijhydene.2009.08.072
7
8
9 Berry AR, Franco CMM, Zhang W, Middelberg APJ (1999) Growth and lactic acid
10 production in batch culture of *Lactobacillus rhamnosus* in a defined medium.
11 *Biotechnol Lett* 21:163–167. doi: 10.1023/A:1005483609065
12
13 Boonmee M, Leksawasdi N, Bridge W, Rogers PL (2003) Batch and continuous culture
14 of *Lactococcus lactis* NZ133: Experimental data and model development. *Biochem*
15 *Eng J* 14:127–135. doi: 10.1016/S1369-703X(02)00171-7
16
17
18 Bruant G, Lévesque MJ, Peter C, Guiot SR, Masson L (2010) Genomic analysis of
19 carbon monoxide utilization and butanol production by clostridium
20 carboxidivorans strain P7T. *PLoS One* 5:1–12. doi: 10.1371/journal.pone.0013033
21
22
23 Burgos-Rubio CN, Okos MR, Wankat PC (2000) Kinetic study of the conversion of
24 different substrates to lactic acid using *Lactobacillus bulgaricus*. *Biotechnol Prog*
25 16:305–314. doi: 10.1021/bp000022p
26
27
28 Cabrol L, Marone A, Tapia-Venegas E, Steyer J-P, Ruiz-Filippi G, Trably E (2017)
29 Microbial ecology of fermentative hydrogen producing bioprocesses: useful
30 insights for driving the ecosystem function. *FEMS Microbiol Rev* 41:158–181.
31 doi: 10.1093/femsre/fuw043
32
33
34 Caporaso JG, Kuczynski J, Stombaugh J, Bittinger K, Bushman FD, Costello EK, Fierer
35 N, Peña AG, Goodrich JK, Gordon JI, Huttley GA, Kelley ST, Knights D, Koenig
36 JE, Ley RE, Lozupone CA, McDonald D, Muegge BD, Pirrung M, Reeder J,
37 Sevinsky JR, Turnbaugh PJ, Walters WA, Widmann J, Yatsunenko T, Zaneveld J,
38 Knight R (2010) QIIME allows analysis of high-throughput community
39 sequencing data. *Nat Methods* 7:335–336. doi: 10.1038/nmeth.f.303
40
41
42 Carrillo-Reyes J, Celis LB, Alatraste-Mondragón F, Razo-Flores E (2014) Decreasing
43 methane production in hydrogenogenic UASB reactors fed with cheese whey.
44 *Biomass and Bioenergy* 63:101–108. doi: 10.1016/j.biombioe.2014.01.050
45
46
47 Cota-Navarro CB, Carrillo-Reyes J, Davila-Vazquez G, Alatraste-Mondragón F, Razo-
48 Flores E (2011) Continuous hydrogen and methane production in a two-stage
49 cheese whey fermentation system. *Water Sci Technol* 64:367–374. doi:
50 10.2166/wst.2011.631
51
52
53
54
55
56
57
58
59
60
61
62
63
64
65

- 1 Davila-Vazquez G, Alatríste-Mondragón F, de León-Rodríguez A, Razo-Flores E (2008)
2 Fermentative hydrogen production in batch experiments using lactose, cheese
3 whey and glucose: Influence of initial substrate concentration and pH. *Int J*
4 *Hydrogen Energy* 33:4989–4997. doi: 10.1016/j.ijhydene.2008.06.065
5
6 Davila-Vazquez G, Cota-Navarro CB, Rosales-Colunga LM, de León-Rodríguez A,
7 Razo-Flores E (2009) Continuous biohydrogen production using cheese whey:
8 Improving the hydrogen production rate. *Int J Hydrogen Energy* 34:4296–4304.
9 doi: 10.1016/j.ijhydene.2009.02.063
10
11 Diekert G, Wohlfarth G (1994) Metabolism of homocetogens. *Antonie Van*
12 *Leeuwenhoek* 66:209–21.
13
14 Dubois M, GILLES KA, HAMILTON JK, REBERS PA, SMITH F (1956) Colorimetric
15 Method for Determination of Sugars and Related Substances. *Anal Chem*
16 28:350–356.
17
18 Edgar RC (2010) Search and clustering orders of magnitude faster than BLAST.
19 *Bioinformatics* 26:2460–2461. doi: 10.1093/bioinformatics/btq461
20
21 Edgar RC, Haas BJ, Clemente JC, Quince C, Knight R (2011) UCHIME improves
22 sensitivity and speed of chimera detection. *Bioinformatics* 27:2194–2200. doi:
23 10.1093/bioinformatics/btr381
24
25 Esquivel-Elizondo S, Chairez I, Salgado E, Aranda JS, Baquerizo G, Garcia-Pe??a EI
26 (2014) Controlled continuous bio-hydrogen production using different biogas
27 release strategies. *Appl Biochem Biotechnol* 173:1737–1751. doi: 10.1007/s12010-
28 014-0961-8
29
30 Etchebehere C, Castelló E, Wenzel J, del Pilar Anzola-Rojas M, Borzacconi L, Buitrón
31 G, Cabrol L, Carminato VM, Carrillo-Reyes J, Cisneros-Pérez C, Fuentes L,
32 Moreno-Andrade I, Razo-Flores E, Filippi GR, Tapia-Venegas E, Toledo-Alarcón
33 J, Zaiat M (2016) Microbial communities from 20 different hydrogen-producing
34 reactors studied by 454 pyrosequencing. *Appl Microbiol Biotechnol* 100:3371–
35 3384. doi: 10.1007/s00253-016-7325-y
36
37 Gomes SD, Fuess LT, Mañunga T, Feitosa de Lima Gomes PC, Zaiat M (2016)
38 Bacteriocins of lactic acid bacteria as a hindering factor for biohydrogen
39 production from cassava flour wastewater in a continuous multiple tube reactor. *Int*
40 *J Hydrogen Energy* 41:8120–8131. doi: 10.1016/j.ijhydene.2015.11.186
41
42 Hung C-H, Cheng C-H, Guan D-W, Wang S-T, Hsu S-C, Liang C-M (2011) Interactions
43 between *Clostridium* sp. and other facultative anaerobes in a self-formed granular
44
45
46
47
48
49
50
51
52
53
54
55
56
57
58
59
60
61
62
63
64
65

- 1
2
3
4
5
6
7
8
9
10
11
12
13
14
15
16
17
18
19
20
21
22
23
24
25
26
27
28
29
30
31
32
33
34
35
36
37
38
39
40
41
42
43
44
45
46
47
48
49
50
51
52
53
54
55
56
57
58
59
60
61
62
63
64
65
- sludge hydrogen-producing bioreactor. *Int J Hydrogen Energy* 36:8704–8711. doi:
10.1016/j.ijhydene.2010.06.010
- Kleerebezem R, Van Loosdrecht MCM (2010) A Generalized Method for
Thermodynamic State Analysis of Environmental Systems. *Crit Rev Environ Sci
Technol* 40:1–54. doi: 10.1080/10643380802000974
- Köpke M, Held C, Hujer S, Liesegang H, Wiezer A, Wollherr A, Ehrenreich A, Liebl W,
Gottschalk G, Dürre P (2010) *Clostridium ljungdahlii* represents a microbial
production platform based on syngas. *Proc Natl Acad Sci* 107:13087–13092. doi:
10.1073/pnas.1004716107
- Kwok JSL, Ip M, Chan T-F, Lam W-Y, Tsui SKW (2014) Draft Genome Sequence of
Clostridium butyricum Strain NOR 33234, Isolated from an Elderly Patient with
Diarrhea. *Genome Announc*. doi: 10.1128/genomeA.01356-14
- Lee J, Jang YS, Han MJ, Kim JY, Lee SY (2016) Deciphering *Clostridium*
tyrobutyricum metabolism based on the whole-genome sequence and proteome
analyses. *MBio* 7:1–12. doi: 10.1128/mBio.00743-16
- Lee K-S, Tseng T-S, Liu Y-W, Hsiao Y-D (2012) Enhancing the performance of dark
fermentative hydrogen production using a reduced pressure fermentation strategy.
Int J Hydrogen Energy 37:15556–15562. doi: 10.1016/j.ijhydene.2012.04.039
- Milferstedt K, Santa-Catalina G, Godon J-J, Escudé R, Bernet N (2013) Disturbance
Frequency Determines Morphology and Community Development in Multi-
Species Biofilm at the Landscape Scale. *PLoS One* 8:e80692. doi:
10.1371/journal.pone.0080692
- Milne CB, Eddy J a, Raju R, Ardekani S, Kim P-J, Senger RS, Jin Y-S, Blaschek HP,
Price ND (2011) Metabolic network reconstruction and genome-scale model of
butanol-producing strain *Clostridium beijerinckii* NCIMB 8052. *BMC Syst Biol*
5:130. doi: 10.1186/1752-0509-5-130
- Napoli F, Olivieri G, Russo ME, Marzocchella Antonio A, Salatino P (2011) Continuous
lactose fermentation by *Clostridium acetobutylicum* - Assessment of acidogenesis
kinetics. *Bioresour Technol* 102:1608–1614. doi: 10.1016/j.biortech.2010.09.004
- Nasr N, Velayutham P, Elbeshbishy E, Nakhla G, El Nagggar MH, Khafipour E,
Derakhshani H, Levin DB, Hafez H (2015) Effect of headspace carbon dioxide
sequestration on microbial biohydrogen communities. *Int J Hydrogen Energy*
40:9966–9976. doi: 10.1016/j.ijhydene.2015.06.077
- Nath K, Das D (2004) Improvement of fermentative hydrogen production: Various

- approaches. *Appl Microbiol Biotechnol* 65:520–529. doi: 10.1007/s00253-004-1644-0
- Noar J, Makwana ST, Bruno-Bárcena JM (2014) Complete Genome Sequence of Solvent-Tolerant *Clostridium beijerinckii* Strain SA-1. *Genome Announc*. doi: 10.1128/genomeA.01310-14
- Noike T, Takabatake H, Mizunoc O, Ohbab M (2002) Inhibition of hydrogen fermentation of organic wastes by lactic acid bacteria. *Int J Hydrogen Energy* 27:1367–1371. doi: 10.1016/S0360-3199(02)00120-9
- Nölling J, Breton G, Omelchenko M V, Kira S, Zeng Q, Gibson R, Lee HM, Dubois J, Qiu D, Hitti J, Sequencing GTC, Wolf YI, Tatusov RL, Sabathe F, Soucaille P, Daly MJ, Bennett GN, Koonin E V, Smith DR (2001) Genome Sequence and Comparative Analysis of the Solvent-Producing Bacterium *Clostridium acetobutylicum* Genome Sequence and Comparative Analysis of the Solvent-Producing Bacterium *Clostridium acetobutylicum*. *J Bacteriol* 183:a823–4838. doi: 10.1128/JB.183.16.4823
- Palomo-Briones R, Razo-Flores E, Bernet N, Trably E (2017) Dark-fermentative biohydrogen pathways and microbial networks in continuous stirred tank reactors: Novel insights on their control. *Appl Energy* 198:77–87. doi: 10.1016/j.apenergy.2017.04.051
- Pyne ME, Utturkar S, Brown SD, Moo-Young M, Chung DA, Chou CP (2014) Improved Draft Genome Sequence of *Clostridium pasteurianum* Strain ATCC 6013 (DSM 525) Using a Hybrid Next-Generation Sequencing Approach. *Genome Announc* 2:2–3. doi: 10.1128/genomeA.00790-14
- R Development Core Team R (2011) R: A Language and Environment for Statistical Computing.
- Rochex A, Godon J, Bernet N, Escudier R (2008) Role of shear stress on composition, diversity and dynamics of biofilm bacterial communities. *Water Res* 42:4915–4922. doi: 10.1016/j.watres.2008.09.015
- Saady NMC (2013) Homoacetogenesis during hydrogen production by mixed cultures dark fermentation: Unresolved challenge. *Int J Hydrogen Energy* 38:13172–13191. doi: 10.1016/j.ijhydene.2013.07.122
- Schuchmann K, Müller V (2014) Autotrophy at the thermodynamic limit of life: a model for energy conservation in acetogenic bacteria. *Nat Rev Microbiol* 12:809–821. doi: 10.1038/nrmicro3365

- 1
2
3
4
5
6
7
8
9
10
11
12
13
14
15
16
17
18
19
20
21
22
23
24
25
26
27
28
29
30
31
32
33
34
35
36
37
38
39
40
41
42
43
44
45
46
47
48
49
50
51
52
53
54
55
56
57
58
59
60
61
62
63
64
65
- Senger RS, Papoutsakis ET (2008) Genome-scale model for *Clostridium acetobutylicum*: Part I. Metabolic network resolution and analysis. *Biotechnol Bioeng* 101:1036–1052. doi: 10.1002/bit.22010
- Shanmugam SR, Chaganti SR, Lalman JA, Heath DD (2014) Statistical optimization of conditions for minimum H₂ consumption in mixed anaerobic cultures: Effect on homoacetogenesis and methanogenesis. *Int J Hydrogen Energy* 39:15433–15445. doi: 10.1016/j.ijhydene.2014.07.143
- Si B, Li J, Li B, Zhu Z, Shen R, Zhang Y, Liu Z (2015) The role of hydraulic retention time on controlling methanogenesis and homoacetogenesis in biohydrogen production using upflow anaerobic sludge blanket (UASB) reactor and packed bed reactor (PBR). *Int J Hydrogen Energy* 40:11414–11421. doi: 10.1016/j.ijhydene.2015.04.035
- Sikora A, Baszczyk M, Jurkowski M, Zielenkiewicz U (2013) Lactic Acid Bacteria in Hydrogen-Producing Consortia: On Purpose or by Coincidence? In: *Lactic Acid Bacteria - R & D for Food, Health and Livestock Purposes*. InTech,
- Sivagurunathan P, Lin C-Y (2016) Enhanced biohydrogen production from beverage wastewater: process performance during various hydraulic retention times and their microbial insights. *RSC Adv* 6:4160–4169. doi: 10.1039/C5RA18815F
- Tracy BP, Jones SW, Fast AG, Indurthi DC, Papoutsakis ET (2012) Clostridia: the importance of their exceptional substrate and metabolite diversity for biofuel and biorefinery applications. *Curr Opin Biotechnol* 23:364–381. doi: 10.1016/j.copbio.2011.10.008

FIGURE CAPTIONS

Fig. 1 Hydrogen production performance of the CSTR operated under different values of OLR. Box plots of VHPR and H₂ yield include all data of the corresponding periods.

a) VHPR and OLR b) H₂ yield and biomass concentration

Fig. 2 Microbial communities and metabolites productivities of dark fermentative systems under different values of OLR. a) Ward D2 hierarchical cluster analysis based on Pearson distances; b) CE-SSCP profiles of microbial communities developed under different OLR; c) VFA and hydrogen yields from steady states. B, butyrate; L, lactate; A, acetate; F, formate

Fig. 3 a) Profiles of the microbial communities from the operation of the CSTR at different conditions of OLR obtained by Illumina MiSeq analysis. b) Relationship between *Clostridium* and *Streptococcus* species with the OLR

Fig. 4 Principal Components Analysis of biohydrogen production under different OLR.

Table 1. Summary of the steady state performance of the dark fermentative CSTR operated under different OLR.

Stage	OLR g _{lactose} /L -d	Theoretical ^a VHPR, L _{H2} /L-d	Experiment al VHPR, L _{H2} /L-d	H ₂ yield mol _{H2} /mol _{Hexose}	H ₂				
					consumed in formate synthesis ^b L _{H2} /L-d	Formate mmol/L	Acetate mmol/ L	Lactate mmol/ L	Butyrate mmol/L
I	88.2	52.4	13.7 ± 1.3	1.21 ± 0.11	5.72	63.9	26.8	33.4	39.6
II	58.8	34.9	5.5 ± 0.3	0.74 ± 0.04	2.01	22.5	19.3	34.1	23.2
III	44.1	26.2	11.6 ± 0.4	2.08 ± 0.12	0.44	5.0	16.9	3.9	30.1
IV	29.4	17.5	7.8 ± 1.1	2.14 ± 0.45	0.25	2.8	8.6	1.0	13.7
V	22.0	13.1	5.5 ± 0.7	1.93 ± 0.23	0.58	6.5	14.6	3.5	24.7
VI	14.7	8.7	3.2 ± 0.7	1.84 ± 0.73	0.54	6.0	8.0	3.7	7.1
VII	58.8	34.9	14.5 ± 0.1	1.90 ± 0.02	1.47	16.4	10.8	49.7	22.3

^aTheoretical VHPR based on the theoretical yield of 4 mol_{H2}/mol_{Hexose} and lactose added.

^bBased on the assumption that formate was produced by the consumption of H₂: CO₂ + H₂ → CHOOH
Samples considered as steady state = 4, 4, 4, 4, 3, 5, and 3 for stages I-VII, respectively.

Table 2. Growth kinetic parameters of representative species of hydrogen producing bacteria and LAB.

Microorganism	Kinetic conditions	μ_{\max} , 1/h	K_S , g/L	Reference
<i>Clostridium acetobutylicum</i>	Lactose, pH 5, 35 °C	0.95	1.34	(Napoli et al. 2011)
<i>Lactococcus casei</i>	Whey-lactose, pH 5.5, 37 °C	0.265	0.72	(Altiok et al. 2006)
<i>Lactobacillus bulgaricus</i>	pH 5.6, 42 °C	1.14	3.36	(Burgos-Rubio et al. 2000)
<i>Lactococcus lactis</i>	Lactose, pH 6.5, 30 °C	1.1	1.32	(Boonmee et al. 2003)
<i>Lactobacillus rhamnosus</i>	Glucose, pH 5.5, 40 °C,	0.45	0.30	(Berry et al. 1999)

Table 3. Gibbs' energy of acetate and formate autotrophic reactions.

	ΔG°	ΔG (Stage VI)	ΔG (Stage I)
$2 \text{HCO}_3^- + 2 \text{H}^+ + 4 \text{H}_2 \rightarrow \text{CH}_3\text{COO}^- + \text{H}^+ + 4 \text{H}_2\text{O}$	-144.4 kJ	-101.2 kJ	-98.15 kJ
$\text{HCO}_3^- + \text{H}^+ + \text{H}_2 \rightarrow \text{CHOO}^- + \text{H}^+ + \text{H}_2\text{O}$	-1.3 kJ	-35.7 kJ	-29.6 kJ

ΔG° were calculated at 25°C and standard concentrations.

ΔG were calculated at pH 5.9, 37°C and the following concentrations: $[\text{HCO}_3^-] = 0.05 \text{ M}$; $[\text{H}_2] = 0.05\text{M}$;

$[\text{VFA}] = \text{Table 1}$.

Gibbs' energy values were computed in accordance with Kleerebezem and Van Loosdrecht (2010).

Figure 1

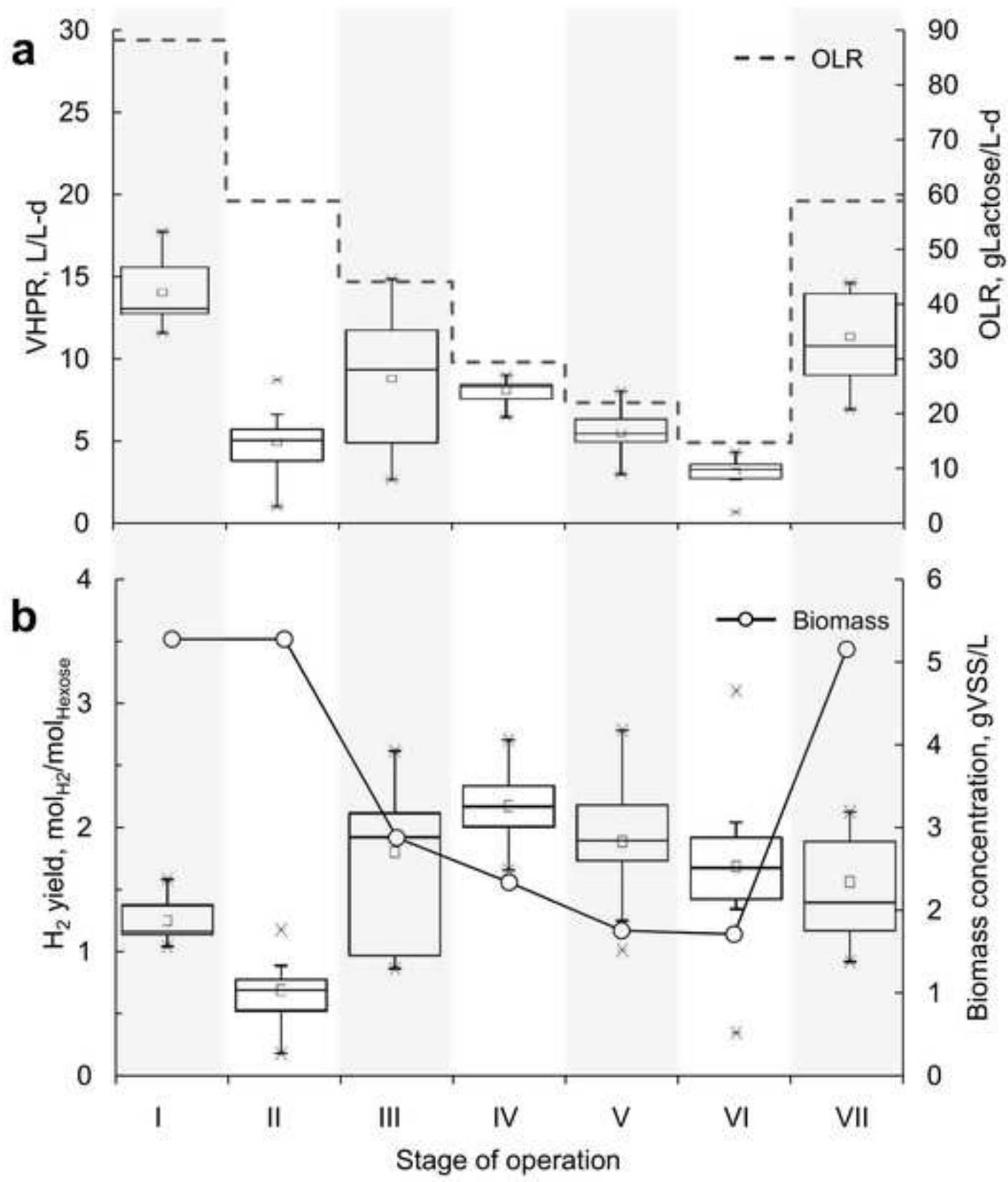
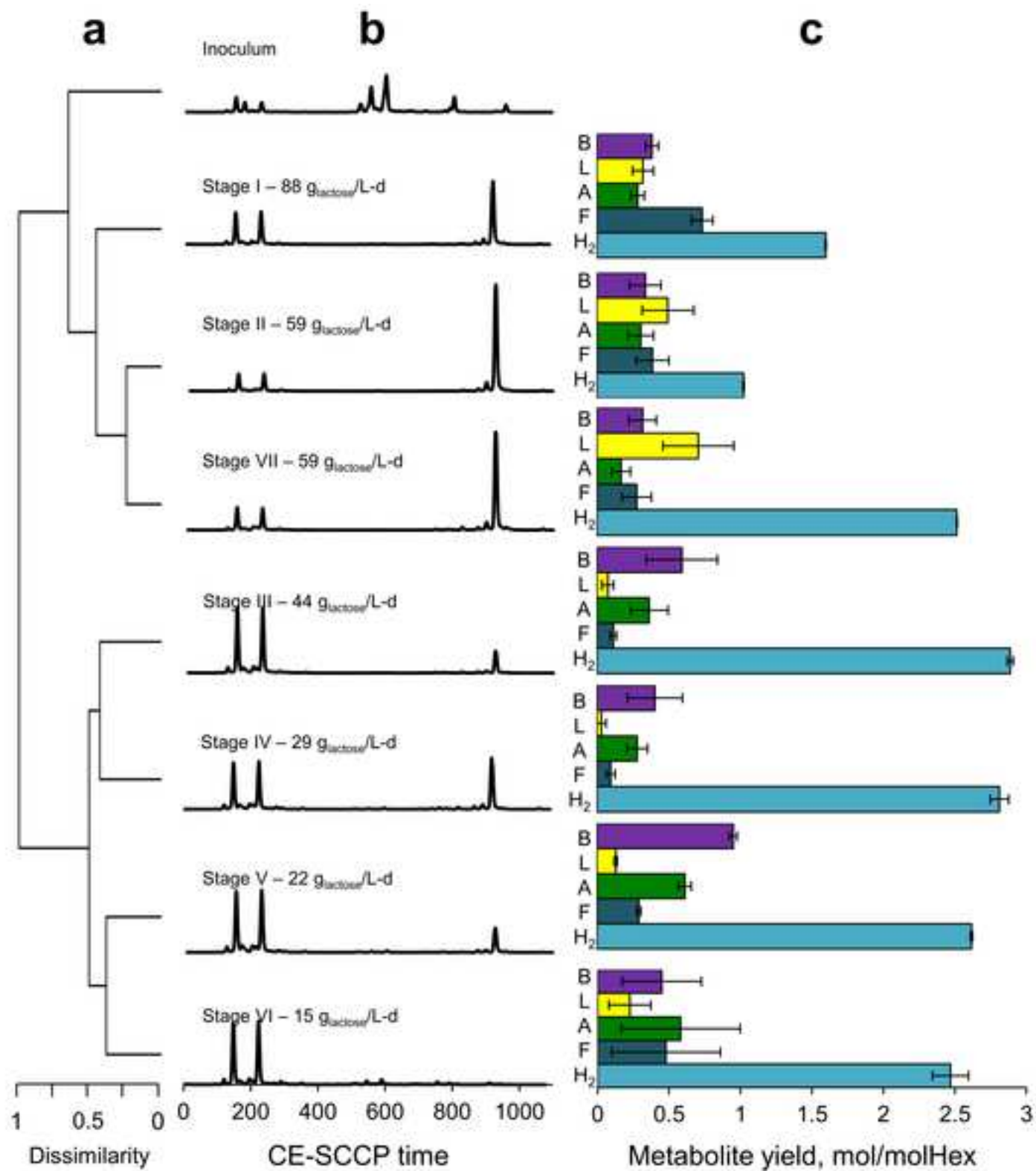


Figure 2



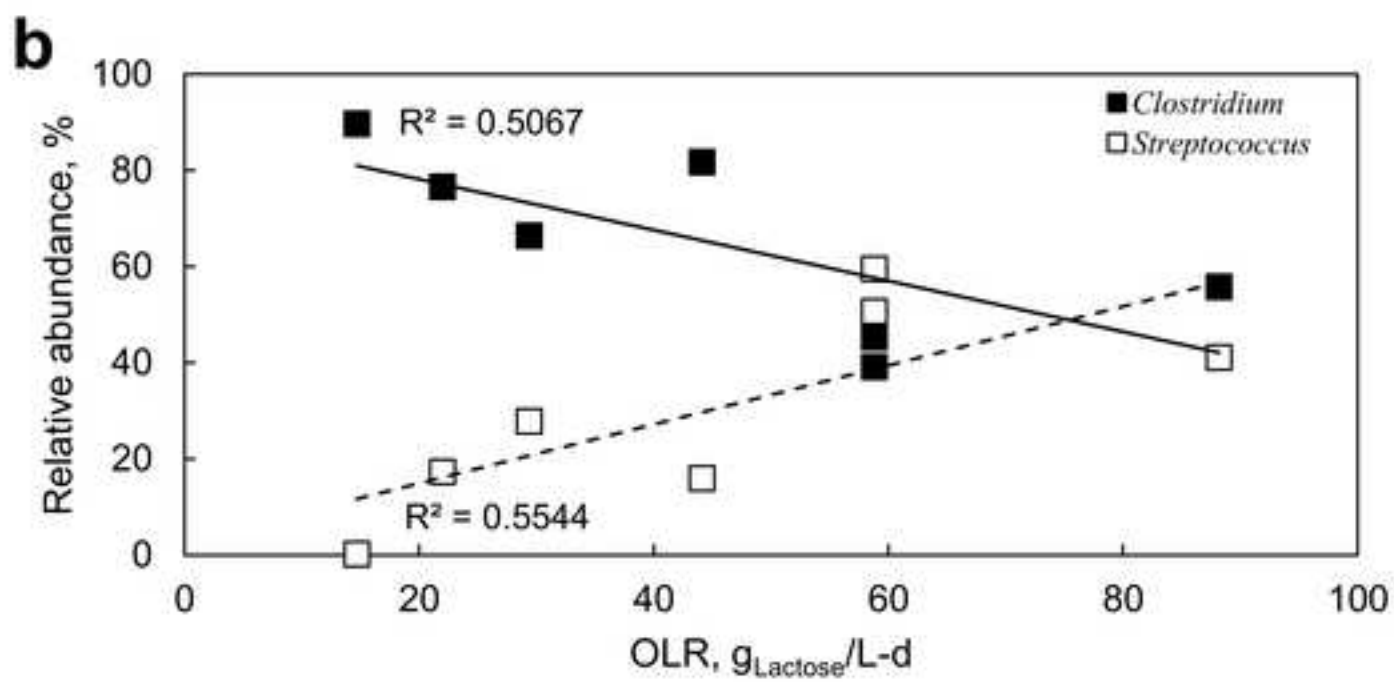
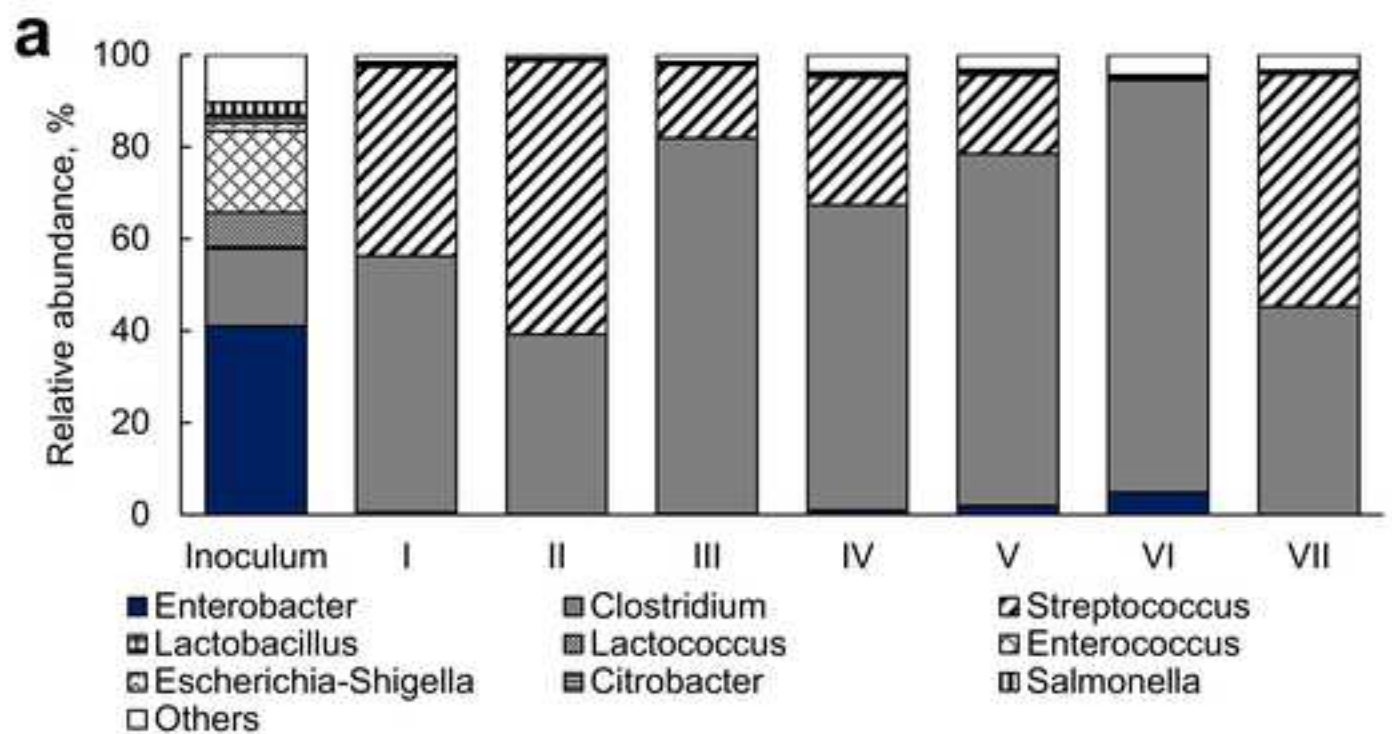


Figure 4

